PG
Petroleum Geoscience

Research article

https://doi.org/10.1144/petgeo2021-060 | Vol. 28 | 2022 | petgeo2021-060

The role of pore pressure and its prediction in deep geothermal energy drilling – examples from the North Alpine Foreland Basin, SE Germany

Michael C. Drews*, Indira Shatyrbayeva, Daniel Bohnsack, Florian Duschl, Peter Obermeier, Markus Loewer, Ferdinand Flechtner and Maximilian Keim

Technical University of Munich, Munich 80333, Germany
MCD, 0000-0002-8461-5576; DB, 0000-0003-0592-4117; FD, 0000-0003-3468-7915; PO, 0000-0002-7754-3703
* Correspondence: michael.c.drews@tum.de
Present address: MCD, Technical University of Munich, Munich 80333, Germany

Abstract: Pore pressure prediction is a well-developed key discipline for well planning in the hydrocarbon industry, suggesting a similar importance for deep geothermal wells, especially, since drilling cost is often the largest investment in deep geothermal energy projects. To address the role of pore pressure prediction in deep geothermal energy, we investigated pore pressure-related drilling problems in the overpressured North Alpine Foreland Basin in SE Germany – one of Europe's most extensively explored deep geothermal energy plays. In the past, pore pressure was mainly predicted via maximum drilling mud weights of offset hydrocarbon wells, but recently more data became available, which led to a re-evaluation of the pore pressure distribution in this area. To compare the impact of pore pressure and its prediction, 70% of all deep geothermal wells drilled have been investigated for pore pressure-related drilling problems and two deep geothermal projects are given as more detailed examples. Thereby, pore pressure-related drilling problems were encountered in one third of all wells drilled, resulting in several side-tracks and an estimated drilling rate decrease of up to 40%, highlighting the importance of accurate pore pressure prediction to significantly reduce the cost of deep geothermal drilling in overpressured environments.

Thematic collection: This article is part of the Geopressure collection available at: https://www.lyellcollection.org/cc/geopressure

Received 27 July 2021; **revised** 24 January 2022; **accepted** 31 January 2022

Deep geothermal energy can contribute to reduce the CO_2 footprint (IRENA 2021) and compared to most other renewable energy forms has the advantage of providing base load capacity and the opportunity to offer clean energy for both electricity generation and district heating (IRENA 2017). Thereby, the technical challenges and associated subsurface risks of deep geothermal energy are closely related to those of classical hydrocarbon exploration and production: finding a producing reservoir, drilling deep wells in sometimes challenging environments, and ensuring safe and sustainable production over timespans of several years to decades. In particular, drilling of deep wells is a significant economic factor in each deep geothermal project and can account for 30–70% of the overall project cost (Stefansson 2002; Stober and Bucher 2013). Consequently, the EU-Commission (2018) has formulated in its strategic energy transition (SET) plan that the cost of drilling for deep geothermal energy (referenced to 2015) has to be reduced by 15% immediately, 30% until 2030 and finally 50% until 2050 to remain competitive on the energy market.

In most cases, the rotary drilling technology is used to drill deep geothermal wells. Here, the deep geothermal industry uses, to a large extent, the experience and technical knowledge built by the hydrocarbon industry (c.f. Stober and Bucher 2013). In the hydrocarbon industry, minimum and maximum drilling fluid densities (mud weight) to prevent kicks, instabilities, sticking and drilling fluid losses as well as designing casing strength and landing points are generally driven by accurate analysis and estimation of pore pressure and subsurface stresses (Mouchet and Mitchell 1989). This task is generally known as pore pressure prediction. Pore pressure prediction is a critical tool to minimize economic, environmental and safety-related drilling risks (e.g. Pinkston and Flemings 2019), but depends on a sufficient database of offset wells (Mouchet and Mitchell 1989). Its significance for drilling hydrocarbon wells suggests a similar importance for deep geothermal wells, which we investigate for the North Alpine Foreland Basin in SE Germany.

The North Alpine Foreland Basin is a low enthalpy (reservoir temperature <200°C) deep geothermal play, which has already completed the transition from being a classical hydrocarbon play in the 1950s to late 1980s (Lemcke 1979; Bachmann *et al.* 1981) into one of Europe's most prolific and most extensively explored deep geothermal (hydrothermal) energy plays (Agemar *et al.* 2014*a*). It also contains a heterogeneous pore pressure distribution with hydrostatic pore pressure, significant overpressure, pressure regressions and underpressure (Lemcke 1976; Müller *et al.* 1988; Drews *et al.* 2018, 2020; Drews and Stollhofen 2019), which makes it an ideal candidate to investigate the role and impact of pore pressure in deep geothermal energy drilling. Moreover, the possible impact of pore pressure prediction on improving drilling performance and lowering drilling cost for the deep geothermal energy sector will be addressed.

North Alpine Foreland Basin in SE Germany

Geological setting

The North Alpine Foreland Basin (referred to NAFB hereafter) is the peripheral foredeep of the European Northern Alps (Schmid

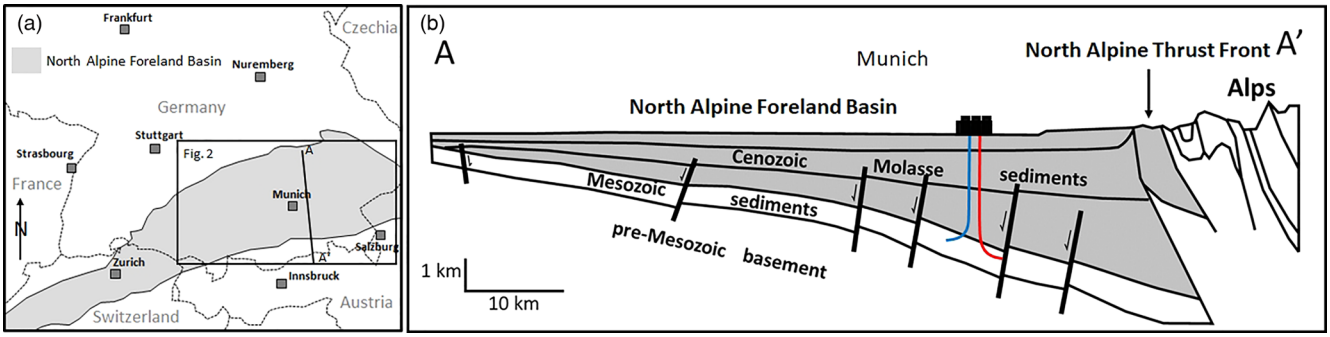

Fig. 1. Geographical and geological overview of the North Alpine Foreland Basin. (**a**) Location of the North Alpine Foreland Basin in SE Germany and Central Europe (modified from Drews *et al.* 2020), (**b**) north–south cross-section (see black line in Fig. 1a) through the North Alpine Foreland Basin modified from Drews *et al.* (2018) after Reinecker *et al.* (2010) and Lüschen *et al.* (2006). The blue and red lines indicate a typical hydrothermal doublet layout with deviated production (red) and injection (blue) wells.

et al. 2004) (Fig. 1a). It originated as a result of continent-continent collision at *c.* 35 Ma (Pfiffner 1986). The SE German part of the NAFB is bounded in the west by Lake Constance and the Austrian border in the east. To the north the Danube River represents the northernmost outline of the NAFB in SE Germany, and the North Alpine Thrust Front marks the southern border of the basin (Schmid *et al.* 2004).

The pre-Mesozoic basement of the NAFB mostly comprises crystalline rocks that formed during the Variscan Orogeny (Bachmann *et al.* 1987). The crystalline basement is covered with mainly Jurassic shales and carbonate rocks, and in the southeastern part, also with carbonate rocks of early Cretaceous age and shales of late Cretaceous age, which in the NW of the basin are partly truncated by an unconformity or completely eroded (Bachmann *et al.* 1987; Allen *et al.* 1991; Bachmann and Müller 1996). Upper Jurassic carbonates, which are the main reservoir for deep geothermal energy production, outcrop at the northern rim of the NAFB, whereas they are buried to depths around 5 km below ground level in front of the Alps (Fig. 1b). Cenozoic basin fill sediments are characterized by two distinct megacycles subdivided into four depositional events (Bachmann and Müller 1996; Sissingh 1997; Kuhlemann and Kempf 2002): the first megacycle starts with deposition of marine shales and marls (early Oligocene) followed by deposition of more terrestrial and coarser grained material (late Oligocene–early Miocene). The second megacycle comprises again finer-grained marine deposits of early Miocene age followed again by terrestrial sediments (middle–late Miocene), respectively. Since the middle to late Miocene, the NAFB in SE Germany was subject to erosion and more recently glaciation and deglaciation. However, total uplift in the undeformed part of the NAFB is believed to amount only to a few hundred meters (Baran *et al.* 2014).

From hydrocarbon to deep geothermal energy production

The NAFB in SE Germany has been extensively explored for hydrocarbons from the 1950s to 1980s (Lemcke 1979; Bachmann *et al.* 1981) with some minor exploration and production activity until recently (Pasternak 2011). Primary targets have been sandstones of Mid Jurassic, Late Cretaceous, Eocene, Oligocene and Miocene depositional ages and carbonates of late Jurassic and Eocene depositional ages (Lemcke 1979). Most thermal water resources have been accidently discovered as a by-product of actual hydrocarbon exploration and usage of thermal water was long limited to hot springs resorts (Schulz *et al.* 2017). In the 1990s, specific deep geothermal energy exploration and production with a focus on district heating began with the shallow projects in the northeastern part of the NAFB in the fractured and karstified carbonates of the Upper Jurassic. The success of these projects further motivated deeper projects in the Upper Jurassic around Munich in the early 2000s (Schulz *et al.* 2017). Also in this time period, the first deep geothermal energy project for electricity generation was realized in Unterhaching (Schulz *et al.* 2017). In the following 10–15 years the Upper Jurassic carbonate reservoir was further developed with successful exploration in and around Munich and the southeastern part of the NAFB in SE Germany (Schulz *et al.* 2017).

Today, 25 deep geothermal projects have found a producible thermal water resource and more projects are planned to be executed in the next years (BVG 2019). Four additional projects did not yield sufficient flow rates and are either abandoned or being further investigated (Fig. 2b). All projects utilize a similar production plan with at least one producer and one injector well (Fig. 1b). Thermal water is exclusively produced from depths between 500 to 5000 mTVD from Upper Jurassic carbonates with flow rates between 30 and 150 l s^{-1} and at temperatures between 60 and 150°C (Agemar *et al.* 2012, 2014*a*, *b*). After heat utilization for electricity generation and/or district heating, the cooled thermal water is reinjected into the reservoir. In total >35 megawatt electrical and >320 megawatt thermal output are currently generated for both electricity generation and district heating, respectively, which is equivalent to >90% of Germany's fully installed deep geothermal power (BVG 2019).

Dataset, methodology and assumptions

Since drilling problems affect sensitive topics such as safety and project economics, all deep geothermal projects have been randomly anonymized with alphanumeric project names from P1 to P29 (Table 1).

The dataset comprises of end of well reports, drilling reports and mud logs from 19 out of 29 deep geothermal projects (Table 1). In addition, drilling histories and/or indications of drilling problems published by Pletl *et al.* (2010); Lackner *et al.* (2018); Fisch *et al.* (2015) and Drews *et al.* (2020) have been used to assess the deep geothermal projects P1, P3, P9 and P14, respectively. In total, drilling and pore pressure relevant data of 80% of all deep geothermal projects (70% of all deep geothermal wells) were available for this study (Table 1).

For all deep geothermal projects except P5 and P19, total measured depth (MD), true vertical depth (TVD) and drilling time (typically spud to rig release) have been retrieved from the geological web map application 'Umweltatlas' of the Bavarian Environment Agency (Bay.LfU 2020) and 2019 version of the NIBIS®Kartenserver (2019). For P5 and P19, information about drilling time was not available.

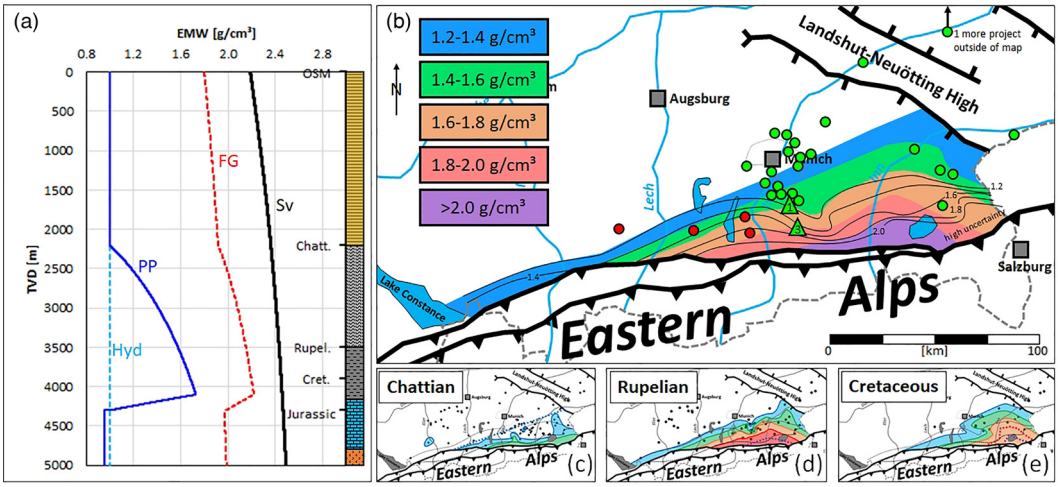

Fig. 2. Pore pressure overview of the North Alpine Foreland Basin in SE Germany. (**a**) Typical vertical pore pressure profile (equivalent mud weight EMW representation) in the overpressured part of the North Alpine Foreland Basin with hypothetical hydrostatic pore pressure (Hyd, dashed light blue line), actual pore pressure (PP, solid blue line), fracture gradient (FG, dashed red line), vertical stress (S_v, black line) and generalized lithological column. Pore pressure and vertical stress were adapted from Drews *et al.* (2018), fracture gradient estimated after Drews *et al.* (2019). (**b**) Maximum pore pressure map in EMW representation. Colours indicate maximum pore pressures based on integrated pore pressure analysis of more than 100 wells (Drews *et al.* 2018), black lines represent maximum drilling mud weights of old hydrocarbon wells (Müller *et al.* 1988). Green and red circles are producible and non-producible deep geothermal projects, respectively. Green triangles indicate location of the producing deep geothermal projects P1 and P3. (**c**)–(**e**) Stratigraphically resolved pore pressures for Upper Oligocene (Chattian), Lower Oligocene (Rupelian) and Upper Cretaceous units (modified from Drews *et al.* 2018).

Table 1. *Anonymized deep geothermal sites with depth ranges, drilling problem type and severity, side-track information and used data sources*

	Max. total depth					
Project	MD [m]	TVD [m]	Primary PP related drilling problems*	Problem severity†	Side-track (ST)?	Data sources‡
P1	>5000	4000–5000	WBS	1	3 drilling problem related ST	Mudlog, Pletl *et al.* (2010)
P2	3000–4000	2000–3000	losses	2		Mudlog
P3	>5000	>5000	kick/influx, DPS	1	3 drilling problem related ST	Lackner *et al.* (2018)
P4	>5000	4000–5000	WBS	1	1 drilling problem related ST	EoWR
P5	4000–5000	3000–4000	unknown	4	1 ST before reaching reservoir	no data
P6	2000–3000	2000–3000	not reported	3		Mudlog
P7	2000–3000	2000–3000	not reported	3		EoWR
P8	3000–4000	3000–4000	WBS	2	1 productivity related ST	EoWR
P9	4000–5000	3000–4000	WBS, losses	1	2 drilling problem related ST	Fisch *et al.* (2015)
P10	<1000	<1000	not reported	3		EoWR
P11	3000–4000	2000–3000	not reported	3		Mudlog
P12	4000–5000	4000–5000	unknown	4	1 productivity related ST	no data
P13	4000–5000	3000–4000	not reported	3		Mudlog
P14	>5000	4000–5000	Kick/influx	1	1 productivity related ST	Drews *et al.* (2020)
P15	2000–3000	2000–3000	Kick/influx	2		EoWR
P16	3000–4000	2000–3000	not reported	3		Mudlog
P17	<1000	<1000	not reported	3	1 productivity related ST	EoWR
P18	2000–3000	2000–3000	unknown	4		no data
P19	>5000	3000–4000	unknown	4	1 ST before reaching reservoir	no data
P20	3000–4000	3000–4000	WBS	2		EoWR
P21	4000–5000	3000–4000	WBS	2		DDR
P22	>5000	4000–5000	kick/influx, DPS	2		EoWR
P23	>5000	4000–5000	WBS	2		DDR
P24	4000–5000	3000–4000	losses	1	1 drilling problem related ST	Mudlog
P25	2000–3000	2000–3000	not reported	3		Mudlog
P26	1000–2000	1000–2000	unknown	4		no data
P27	4000–5000	3000–4000	WBS	2	1 productivity related ST	EoWR
P28	3000–4000	3000–4000	WBS	1	1 drilling problem related ST	EoWR
P29	3000–4000	2000–3000	unknown	4		no data

*WBS, wellbore stability (cavings, tight spots, repeated overpulls); DPS, differential pressure sticking.
†1 = major, 2 = minor/negligible, 3 = none/not reported, 4 = unknown.
‡EoWR, end of well report; DDR, daily drilling reports.

Classification of drilling problems

Reported drilling problems have been classified into *major* and *minor/negligible* problems. *Major* drilling problems resulted in either side-track operations, significant kicks or both. *Minor/negligible* drilling problems represent events which have been noticed, but did not significantly impede the drilling operations (including minor influxes). Wells without any reported drilling problems are labelled as *none/not reported* (Table 1).

Estimation of drilling rate

Drilling rate per project is estimated in average project drilling depth (in meters) per time (in hours) averaged over the number of wellbores, exclusive of any side-tracks, to reach the reservoir target. Drilling hours per project are rounded to the cumulative full day's difference between drilling start and drilling end as published by the Bavarian Environmental Agency (Bay.LfU 2020) and NIBIS®Kartenserver (2019) of each well, but again exclusive of side-tracks which were drilled to enhance the reservoir performance. Drilling time can however be inclusive of production testing and other technical problems (e.g. power outage, weather, chemical mud reactions, etc.) all of which bias the drilling rate estimate towards lower values – in particular for shallower wells.

To showcase the drilling rate estimate we assume a deep geothermal project with two wells. The first well drilled in 60 days to 3000 mMD, then required a side-track due to pore pressure-related drilling problems from 2700 mMD and reached the target at 4000 mMD after another 30 days. The second well reached the target at 4200 mMD after 80 days and subsequently drilled a side-track from 3500 to 4500 mMD to enhance reservoir performance, which took another 15 days. In that case, the cumulative drilling days would amount 170 days and the average measured drilling depth for the project would be 4100 mMD. The resulting average drilling rate for both wells would therefore be 2.01 meters per hour ($m\ h^{-1}$).

Since the retrieved drilling rate only provides a rough estimate and not an exact representation of the drilling progress, we normalized all drilling rates to the highest (fastest) drilling rate of all projects.

Review of pore pressure prediction and distribution in the NAFB

The NAFB in SE Germany displays a complex pore pressure distribution (Fig. 2) with pressure ramps and a pressure regression in its overpressured parts (Fig. 2a). Until recently, pore pressure prediction for deep geothermal drilling was mainly guided by maximum drilling mud weights from old hydrocarbon wells (Müller *et al.* 1988) (Fig. 2b, black lines) due to limited digital data availability and access. The limited data availability led to significant drilling problems in step-out projects as reported for example for the deep geothermal projects P1 (Pletl *et al.* 2010) and P3 (Lackner *et al.* 2018) (Fig. 2b). Recent access to and digitization of geophysical well log data, vertical seismic profiles, geological well tops and pressure tests of hydrocarbon wells and deep geothermal wells facilitated a reinterpretation of the pore pressure distribution (Drews *et al.* 2018). As a result, stratigraphically resolved pore pressure gradient maps have been established suggesting that the overpressure zone is likely much more extensive (Drews *et al.* 2018) (Fig. 2b–e). In addition, the lateral pore pressure distribution most likely follows a different spatial trend in the southeastern part of the NAFB, but this area is also marked by the highest uncertainty due to limited data availability (Fig. 2b).

This reinterpretation, together with previous studies (Lemcke 1976; Müller *et al.* 1988), yielded a more detailed and holistic understanding of the distribution of pore pressure in the NAFB: Upper Jurassic carbonates exhibit extremely well developed hydraulic connectivity due to faulting, karstification and dolomitization (Birner 2013; Böhm *et al.* 2013; Budach *et al.* 2018; Bohnsack *et al.* 2020). Since Upper Jurassic carbonates crop out at the northern rim of the basin, and due to their exceptional hydraulic properties, the hydraulic head within the aquifer generally follows that of the Danube River (Lemcke 1976), which flows from west to east. As a consequence, pore pressure in the Upper Jurassic is generally (sub-)hydrostatic (Fig. 2a) and slightly decreasing from west to east. Lower Cretaceous carbonates, if present, share the same pressure regime with Upper Jurassic carbonates (Lemcke 1976; Drews *et al.* 2020).

Pore pressure of the Cenozoic basin fill appears to be dependent on several factors: a) deposition of low permeability marine sediments such as shales and marls, b) elevated subsidence and sedimentation rates during late Oligocene and early Miocene and c) presence of Upper Cretaceous shales, which act as hydraulic barrier between the Cenozoic basin fill and sub-hydrostatically pressured Lower Cretaceous and Upper Jurassic passive margin carbonates (Müller *et al.* 1988; Drews *et al.* 2018, 2020). Marine deposits, high sedimentation rates in excess of 200 m myr^{-1} and Upper Cretaceous shales are all present in the south and southeastern parts of the NAFB in SE Germany (c.f. Bachmann *et al.* 1987; Zweigel 1998; Kuhlemann and Kempf 2002; Drews *et al.* 2020). Here, overpressure starts to develop below 1500–2500 m in Chattian marls and shales and usually reaches pore pressure gradients up to 2.0 g cm^{-3} in equivalent mud weight (EMW) representation in sediments of lower Rupelian depositional age (Müller *et al.* 1988; Drews *et al.* 2018) (Fig. 2a–d). In the very southeastern part of the basin, peak pore pressure gradients in excess of 2.0 g cm^{-3} EMW were encountered in Upper Cretaceous shales (Müller *et al.* 1988; Drews *et al.* 2018) (Fig. 2e), which reach a thickness >400 m in this area (Bachmann *et al.* 1987; Przybycin *et al.* 2017).

Velocity and vertical effective stress-based analysis of shale pore pressure as well as 3D basin modelling indicate that overpressure is mostly generated by vertical loading and disequilibrium compaction (Drews *et al.* 2018, 2020). However, clay diagenesis has been reported in the Austrian part of the basin (Gier *et al.* 1998) and could also contribute to overpressure generation. Similarly, hydrocarbon generation and oil-to-gas cracking might be an additional source of overpressure in very organic matter-rich formations. In particular, the lower Rupelian comprises a section of high organic matter content (Bachmann *et al.* 1987; Sachsenhofer *et al.* 2010).

Furthermore, the effect of tectonic stress on overpressure generation is most likely increasing with decreasing distance to the North Alpine Thrust Front (Drews *et al.* 2020; Müller *et al.* 1988). Tectonic stress probably also results in elevated differential horizontal stresses, which might additionally facilitate drilling problems due to breakouts. Breakouts have been recorded in most hydrocarbon wells and indicate a predominant orientation of the maximum horizontal stress perpendicular to the North Alpine Thrust Front (Reinecker *et al.* 2010).

The reinterpretation of the pore pressure distribution now allows for a stratigraphically resolved pore pressure prediction with less uncertainty, since various data sources (direct pressure tests and indicators, drilling events, mud weight profiles and shale compaction) have been incorporated. The reinterpretation also points at areas, where underbalanced drilling was likely a common practice, in particular during the early stage of hydrocarbon exploration. In these areas, the pore pressure estimate based on maximum drilling mud weights (Müller *et al.* 1988) significantly differs from the reinterpreted pore pressure magnitudes (Drews *et al.* 2018) (compare black isobars with colour-coded isobars on Fig. 2b).

Pore pressure-related drilling problems

As described above, pore pressure models for well planning often followed published maximum drilling mud weights of old hydrocarbon wells (Müller *et al.* 1988) and past experience from other geothermal wells, which can be far away from the actual drilling location. Although maximum drilling mud weights give a first order orientation of the distribution of pore pressure in the NAFB, they reflect the style of drilling and the driller's perception of pore pressure at the time rather than an integrated analysis of pore pressure utilizing various data sources. The lack of pore pressure data, except for maximum drilling mud weights of old hydrocarbon wells, has often led to underbalanced drilling and subsequent significant drilling problems in deep geothermal wells (Table 1). In fact, more than half of all deep geothermal projects or one third of all geothermal wells drilled in the NAFB experienced geological drilling problems (Fig. 3a, b). The vast majority of these wells were drilled through the overpressured zone, and all of the reported problems are related to either kicks, wellbore instabilities (collapse, cavings, tight spots, etc.) or differential pressure sticking or losses due to previously increased mud weight (Fig. 3c, Table 1).

Wellbore stability is additionally challenging, since the kick-off point for highly deviated drilling, which is standard to maximize the production zone in the reservoir, is usually on top or within the pore pressure ramp (e.g. Lackner *et al.* 2018). Also, significant impact of tectonic stress on both overpressure generation and wellbore shear failure (breakouts) can be expected in a foreland basin setting such as the NAFB. The large amount of wellbore stability problems in deep geothermal wells and previously recorded breakouts in hydrocarbon wells (Reinecker *et al.* 2010) support this hypothesis. However, since many of these wells have likely been drilled underbalanced, formation of large breakouts and washouts does not necessarily require large differential horizontal stresses (c.f. Fjaer *et al.* 2008). The detailed analysis of wellbore failure and elevated differential horizontal stresses could therefore further improve drilling performance in the NAFB.

For almost one quarter of all projects (or 14% of all wells) the described challenges resulted in major drilling problems such as significant kicks, side-track operations or both (Fig. 3a, b and d) and problems occurred more often in deeper projects/wells than shallower ones (Fig. 3d). Still, these numbers represent the lower boundary since no data was available for one fifth of all projects (or 30% of all wells) to investigate pore pressure-related drilling problems. Besides, most wells with 'none/not reported' drilling problems only had a mud log available as data source (Table 1), which rarely report minor drilling problems.

In total, 11 side-tracks had to be drilled due to geological drilling problems, which are likely related to abnormal pore pressures (Table 1). On top of that, two more side-tracks likely fall in this category, too, since side-track operations started before reaching the reservoir. However, no data was available for the respective projects. The occurrence of pore pressure-related drilling problems also correlates with the overall project depth (Fig. 3d), since within the overpressure zone pore pressure increases with increasing depth (Fig. 4a). Comparing pore pressure estimates from maximum drilling mud weights (Müller *et al.* 1988) with more recent pore pressure estimates which integrated drilling, geophysical and geological data (Drews *et al.* 2018, 2020) suggests most wells with drilling problems would be drilled significantly underbalanced, if planned on an offset maximum drilling mud weight basis only (Fig. 4b), which provides an explanation for the experienced drilling challenges.

The impact of pore pressure prediction can be additionally exemplified by two deep geothermal projects which experienced

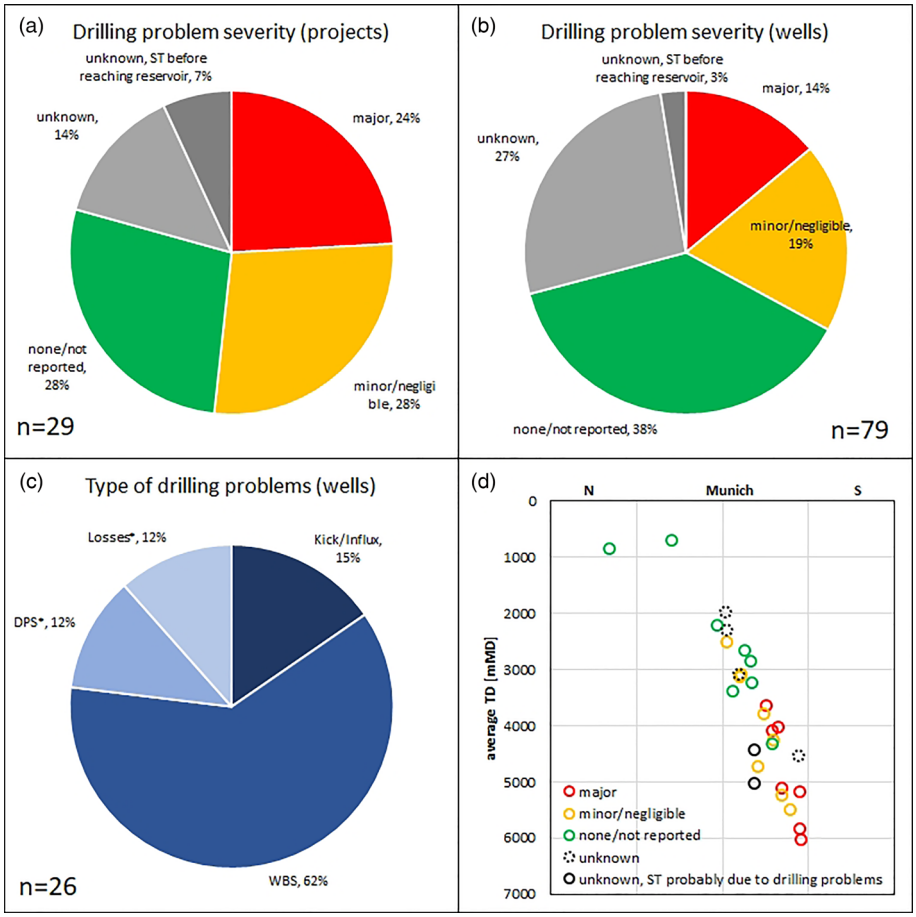

Fig. 3. Overview of pore pressure-related drilling problems. (**a**) Pie chart showing the percentages of deep geothermal projects with major or minor/negligible drilling problems, (**b**) same as A, but for individual wells, (**c**) subset of wells with drilling problems showing the fractions of wells with different drilling problems (WBS refers to either wellbore stability, collapse, severe cavings or a combination; DPS is short for differential pressure sticking). Drilling fluid losses (Losses*) only includes those incidences which led to side-tracks, (**d**) all deep geothermal projects represented in geographical Northing v. average total drilling depth (measured depth MD) after Flechtner and Aubele (2019). Colour-coding indicates severity of drilling problems according to Figure 3a, b.

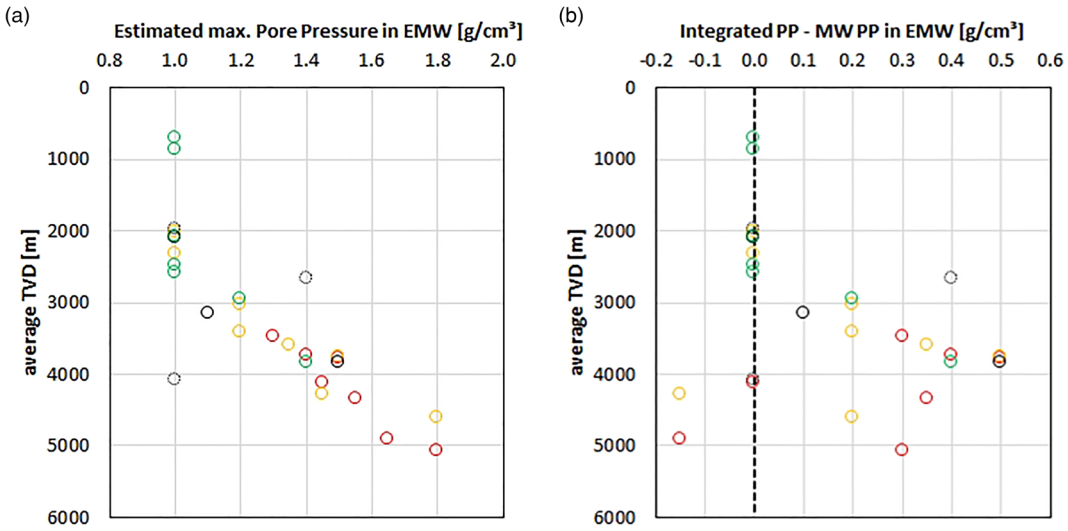

Fig. 4. Relation between pore pressure and drilling problems for all deep geothermal projects. Colour-coding represents drilling problem severity (red = major, yellow = minor/negligible, green = none/not reported, dotted black = unknown). (**a**) Estimated maximum pore pressure (after Drews *et al.* 2018; c.f. Fig. 2b) v. average true vertical depth, (**b**) average true vertical depth of each deep geothermal project v. the difference between predicted pore pressure based on integrated pore pressure estimation (after Drews *et al.* 2018) and maximum drilling mud weights of offset wells only (after Müller *et al.* 1988) – also compare with Figure 2b above.

significant drilling problems with subsequent side-track operations. These two projects are the deep geothermal projects P1 and P3 (see Fig. 2b for project locations), whose drilling problems have been reported, revisited and published in retrospect by Pletl *et al.* (2010) and Lackner *et al.* (2018), respectively. Both deep geothermal projects are extreme cases for pore pressure-related drilling problems and were the first step-outs into the overpressure zone southward of Munich. Both projects therefore provide valuable case studies and reference cases highlighting the importance of an integrated pore pressure analysis and prediction in deep geothermal exploration drilling.

Deep geothermal project P1 was drilled in 2007 to a maximum total depth of 5567 mMD and experienced severe drilling problems, presumably due to heavy pressure cavings in the Lower Rupelian shales (Pletl *et al.* 2010). These problems led to two side-tracks and to *c.* 50% of additional drilling time (Pletl *et al.* 2010). High pore pressures were not anticipated and indeed offset maximum drilling mud weights indicate only very mild overpressures of around 1.2 g cm^{-3} in EMW (Müller *et al.* 1988) (Figs 2b, 5b). The reinterpreted pore pressure distribution (Drews *et al.* 2018) (Fig. 2b) however reveals a different picture: Pore pressures of up to 1.5–1.6 g cm^{-3} EMW in the trouble zone of the Lower Rupelian seem to be much more likely and offer an explanation of the experienced drilling problems (Fig. 5b). According to the mud log of the last P1 well, the trouble zone was finally drilled with a mud weight of 1.45 g cm^{-3}.

Deep geothermal project P3 was executed in 2016 and reached a maximum total depth of 6084 mMD (Lackner *et al.* 2018). The first well experienced a strong gas kick in sandstones of the Lower Rupelian, which led to a first side-track (Lackner *et al.* 2018). For the second well, mud weight was apparently increased to compensate for the elevated pressures in the kick zone, but resulted in differential pressure sticking in sands of Chattian age and two more side-tracks (Lackner *et al.* 2018). In total, drilling time almost doubled for deep geothermal project P3 due to the reported pore pressure-related drilling problems (Lackner *et al.* 2018). Anticipated pore pressure based on maximum drilling mud weights from offset hydrocarbon wells indicate a maximum pore pressure of 1.5 g cm^{-3} EMW (Müller *et al.* 1988) (Figs 2b, 5b), while the reinterpreted pore pressure distribution (Drews *et al.* 2018) (Fig. 2b) indicates a mud weight of at least 1.8 g cm^{-3} would be required (Figs 2b, 5b).

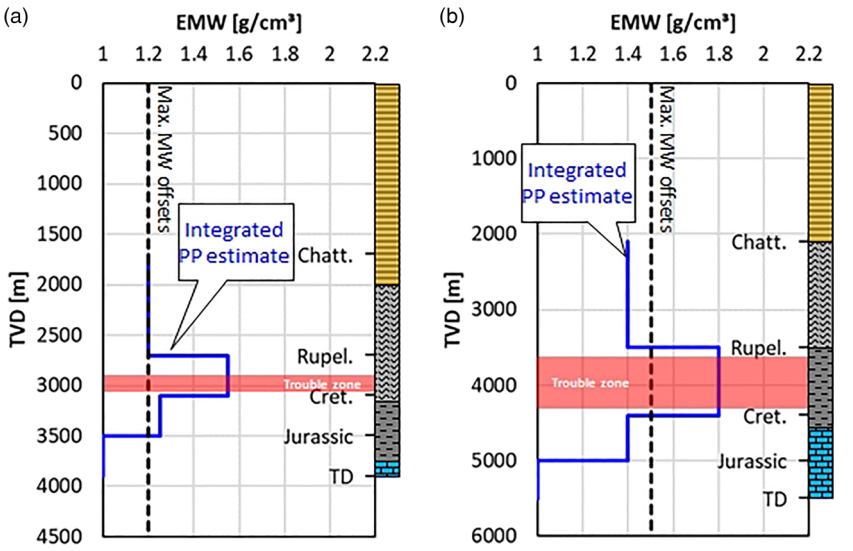

Fig. 5. Examples for the impact of integrated pore pressure analysis on drilling performance. (**a**) Vertical profile of deep geothermal project P1 (see green triangle '1' on Fig. 2b for location) with trouble zone (red transparent rectangle) with severe wellbore collapse. Tops and trouble zone depths and stratigraphy from Pletl *et al.* (2010). (**b**) Vertical profile of deep geothermal project P3 (see green triangle '3' on Fig. 2b for location) with trouble zone (red transparent box) with strong gas kick. Tops from a nearby hydrocarbon offset well (Well C in Drews *et al.* 2020) and trouble zone depth and trouble zone stratigraphy from Lackner *et al.* (2018). (a) & (b): pore pressure estimate based on maximum drilling mud weights of offset wells (black dashed line) after Müller *et al.* (1988) and simplified reinterpreted pore pressure profile (blue line) after Drews *et al.* (2018).

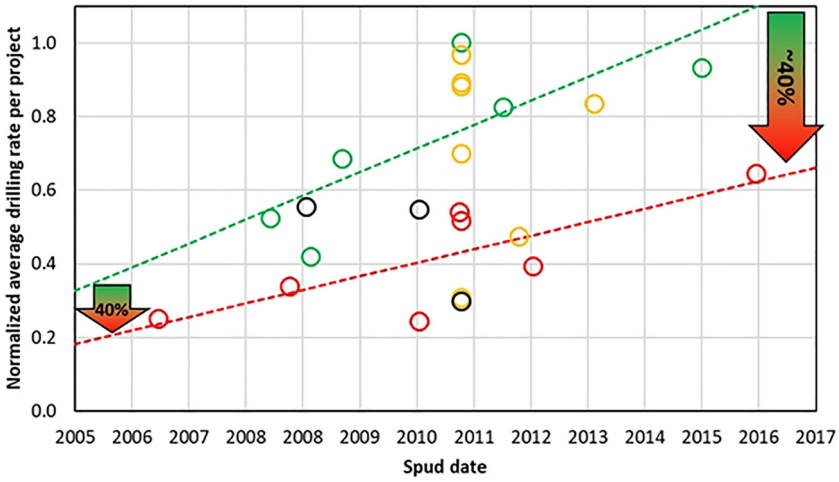

Fig. 6. Normalized average drilling rate per deep geothermal project as a function of the spud date. Colour-coding represents drilling problem severity (red = major, yellow = minor/negligible, green = none/not reported, black = unknown). No drilling rates have been calculated for projects P5 and P19. The green and red dashed line indicate the average drilling rate improvement over time for projects which experienced none/not reported and major drilling problems, respectively. For the latter, drilling rate is approximately reduced by 40% at all times (c.f. green-red coloured arrows).

Drilling rate and drilling cost v. pore pressure related drilling problem severity

Usually, the cost of drilling amounts between 30–70% of the overall project cost (e.g. Stefansson 2002; Stober and Bucher 2013). The impact of non-productive time due to pore pressure-related drilling problems can therefore be significant for the entire project economics. Standardized drilling rates in mMD per hour have been calculated using cumulated rig time (typically spud to rig release) and average total measured depth for all wells of each project, excluding side-tracks. No drilling rates have been calculated for the projects P10 and P17, where maximum drilling depth did not exceed 1000 mTVD (Table 1). Here, the impact of testing on overall rig time is particularly high due to the short drilling time, which would result in unrealistically slow drilling rates.

Figure 6 shows normalized estimated drilling rate as a function of the spud date and drilling problem severity (*major*, *minor/negligible*, *none/not reported*). Drilling rates increase over time for projects which experienced *none/not reported* and *major* drilling problems, reflecting the general learning curve of deep geothermal drilling in the NAFB. Projects with *minor/negligible* drilling problems do not follow a drilling rate trend over time, which is related to the narrow time range covered by the respective projects and a larger spread in drilling rates.

On average, drilling rates of projects with *major* pore pressure related drilling problems are *c.* 40% lower than projects with *none/not reported* drilling problems (Fig. 6). Assuming the actual drilling process accounts for *c.* 50% of the overall cost of a deep geothermal well (c.f. Augustine *et al.* 2006), avoidance of pore pressure related drilling problems can result in a cost saving of up to 20% in the NAFB. This alone can already exceed or significantly contribute to the EU-SET plan goals to reduce drilling costs (compared to 2015) by 15% (immediately), 30% (by 2030) and 50% (by 2050) (EU-Commission 2018). Attributing a maximum of 70% of total deep geothermal project costs to drilling (c.f. Stefansson 2002; Stober and Bucher 2013), accurate pre-drill pore pressure prediction and analysis could therefore reduce the total developing cost of an entire geothermal play with similar overpressure settings by 10–20%.

Conclusions

Pore pressure-related drilling problems in the context of deep geothermal exploration drilling have been investigated on a regional scale for the deep geothermal energy play in the abnormally pressured North Alpine Foreland Basin, SE Germany.

The drilling problems have been set into context with different previously published pore pressure estimates in the study area: (1) based on maximum drilling mud weights of old hydrocarbon wells and (2) integrated pore pressure prediction/analysis incorporating drilling, pressure test, geophysical and geological data. Thereby, drilling problems correlate with an underestimation of pore pressure magnitudes on the basis of offset maximum drilling mud weights. Hereby, more than 50% of all projects or one third of all wells drilled experienced minor or major pore pressure-related drilling issues. The actual percentage is likely even higher, since not all wells investigated had a full data set available and 30% of the wells have not been investigated due restricted data access at the time of this study.

A large amount of drilling challenges is attributed to wellbore stability problems. The detailed analysis of wellbore failure due to elevated tectonic stress should therefore be a future field of research to further improve drilling performance in the NAFB.

On average, major pore pressure related drilling problems result in a 40% decrease of drilling rate and thus significantly impact project economics. Averaged over all deep geothermal projects in a deep geothermal play, a fully integrated pre-drill pore pressure analysis/prediction can potentially reduce drilling cost by up to 20% in overpressured basins like the North Alpine Foreland Basin in SE Germany. This alone can significantly contribute to the EU-SET plan goals to reduce drilling costs of deep geothermal energy projects.

The demonstrated impact of accurate pre-drill pore pressure prediction on drilling performance and cost equally provides a useful real-world example for project developers and management of the petroleum and deep geothermal energy industry. Finally, an improved pore pressure prediction will make the petroleum and deep geothermal energy industries safer for drilling crews and contributes to reduction of the risk of environmental damage caused by well control incidents.

Acknowledgements The authors would like to thank the deep geothermal operators who provided data to investigate pore pressure related drilling problems. In addition, the authors like to acknowledge the collaboration with the Bavarian Environment Agency for their support to access additional data sets of deep geothermal and hydrocarbon wells in the study area. The authors thank Toby Harrold and an anonymous reviewer for their suggestions and comments, which greatly helped to improve the readability and quality of the manuscript.

Author contributions **MCD**: conceptualization (lead), data curation (lead), formal analysis (lead), funding acquisition (lead), investigation (lead), methodology (lead), project administration (equal), writing – original draft (lead), writing – review & editing (lead); **IS**: data curation (equal), investigation (equal), writing – review & editing (equal); **DB**: data curation (equal), investigation (equal), writing – review & editing (equal); **FD**: investigation (equal), writing – review & editing (equal); **PO**: investigation (equal), writing – review & editing (supporting); **ML**: data curation (equal), project administration (equal), writing – review & editing (supporting); **FF**: conceptualization (equal), data curation (equal), investigation (equal), writing – review & editing (supporting); **MK**: data curation (equal), project administration (lead), writing – review & editing (equal)

Funding The authors would like to thank the Bavarian State Ministry of Science and the Arts, which funded the study and database acquisition in the framework of the Geothermal-Alliance Bavaria (GAB).

Data availability The data that support the findings of this study are available from deep geothermal operators in Bavaria and Geothermal-Alliance Bavaria but restrictions apply to the availability of these data, which were used under licence for the current study, and so are not publicly available. Data are however available from the authors upon reasonable request and with permission of deep geothermal operators in Bavaria and Geothermal-Alliance Bavaria.

Competing interests The authors declare that they have no known competing financial interests or personal relationships that could have appeared to influence the work reported in this paper.

References

Agemar, T., Schellschmidt, R. and Schulz, R. 2012. Subsurface temperature distribution in Germany. *Geothermics*, **44**, 65–77, https://doi.org/10.1016/j.geothermics.2012.07.002

Agemar, T., Weber, J. and Schulz, R. 2014*a*. Deep geothermal energy production in Germany. *Energies*, **7**, 4397–4416, https://doi.org/10.3390/en7074397

Agemar, T., Alten, J., Ganz, B., Kuder, J., Kühne, K., Schumacher, S. and Schulz, R. 2014*b*. The Geothermal Information System for Germany - GeotIS. *ZDGG*, **165**, 129–144, https://doi.org/10.1127/1860-1804/2014/0060

Allen, P.A., Crampton, S.L. and Sinclair, H.D. 1991. The inception and early evolution of the north Alpine foreland basin, Switzerland. *Basin Research*, **3**, 143–163, https://doi.org/10.1111/j.1365-2117.1991.tb00124.x

Augustine, C., Tester, J.W., Anderson, B., Petty, S. and Livesay, B. 2006. A comparison of geothermal with oil and gas well drilling costs. Proceedings of the Thirty-First Workshop on Geothermal Reservoir Engineering, Stanford University, Stanford, CA, USA, 15.

Bachmann, G.H. and Müller, M. 1996. Die Entwicklung des süddeutschen Molassebeckens seit dem Variszikum: Eine Einführung. *Zeitschrift für Geologische Wissenschaften*, **24**, 3–20.

Bachmann, G.H., Koch, K., Müller, M. and Weggen, K. 1981. Ergebnisse und Erfahrungen bei der Exploration in den Bayerischen Alpen. *Erdoel-Erdgas-Zeitschrift*, **97**, 127–133.

Bachmann, G.H., Müller, M. and Weggen, K. 1987. Evolution of the Molasse Basin (Germany, Switzerland). *Tectonophysics*, **137**, 77–92, https://doi.org/10.1016/0040-1951(87)90315-5

Baran, R., Friedrich, A.M. and Schlunegger, F. 2014. The late Miocene to Holocene erosion pattern of the Alpine foreland basin reflects Eurasian slab unloading beneath the western Alps rather than global climate change. *Lithosphere*, **6**, 124–131, https://doi.org/10.1130/L307.1

Bay.LfU 2020. *Umweltatlas*. Bayerisches Landesamt für Umwelt.

Birner, J. 2013. *Hydrogeological Model of the Malm Aquifer in the South German Molasse Basin*. PhD, Freie Universität Berlin.

Böhm, F., Savvatis, A., Steiner, U., Schneider, M. and Koch, R. 2013. Lithofazielle Reservoircharakterisierung zur geothermischen Nutzung des Malm im Großraum München. *Grundwasser – Zeitschrift der Fachsektion Hydrogeologie*, **18**, 3–13, https://doi.org/10.1007/s00767-012-0202-4

Bohnsack, D., Potten, M., Pfrang, D., Wolpert, P. and Zosseder, K. 2020. Porosity–permeability relationship derived from Upper Jurassic carbonate rock cores to assess the regional hydraulic matrix properties of the Malm reservoir in the South German Molasse Basin. *Geothermal Energy*, **8**, https://doi.org/10.1186/s40517-020-00166-9

Budach, I., Moeck, I., Lüschen, E. and Wolfgramm, M. 2018. Temporal evolution of fault systems in the Upper Jurassic of the Central German Molasse Basin: case study Unterhaching. *International Journal of Earth Sciences*, **107**, 635–653, https://doi.org/10.1007/s00531-017-1518-1

BVG 2019. Tiefe Geothermie-Projekte in Deutschland 2019, https://www.geothermie.de/fileadmin/user_upload/Bibliothek/Downloads/Poster_TG-Projekte_in_Deutschland_2019.pdf [last accessed 17 June 2021].

Drews, M. and Stollhofen, H. 2019. PPFG prediction in complex tectonic settings: the north Alpine Thrust Front and Foreland Basin, SE Germany. presented at the Second EAGE Workshop on Pore Pressure Prediction, 19 May 2019, Amsterdam.

Drews, M.C., Bauer, W., Caracciolo, L. and Stollhofen, H. 2018. Disequilibrium compaction overpressure in shales of the Bavarian Foreland Molasse Basin: results and geographical distribution from velocity-based analyses. *Marine and Petroleum Geology*, **92**, 37–50, https://doi.org/10.1016/j.marpetgeo.2018.02.017

Drews, M.C., Seithel, R., Savvatis, A., Kohl, T. and Stollhofen, H. 2019. A normal-faulting stress regime in the Bavarian Foreland Molasse Basin? New evidence from detailed analysis of leak-off and formation integrity tests in the greater Munich area, SE-Germany. *Tectonophysics*, **755**, 1–9, https://doi.org/10.1016/j.tecto.2019.02.011

Drews, M.C., Hofstettter, P., Zosseder, K., Shipilin, V. and Stollhofen, H. 2020. Predictability and mechanisms of overpressure in the Bavarian Foreland Molasse Basin: an integrated analysis of the Geretsried GEN-1 deep geothermal well. *Geothermal Energy*, **8**, 20, https://doi.org/10.1186/s40517-020-00175-8

EU-Commission 2018. *SET Plan Delivering Results: The Implementation Plans,* European Union, 56.

Fisch, H., Uhde, J., Bems, C., Lang, P. and Bartels, J. 2015. Hydraulic testing and reservoir characterization of the Taufkirchen site in the Bavarian Molasse Basin, Germany. World Geothermal Congress, 19–25 April 2015, Melbourne, Australia, 1–14.

Fjaer, E., Holt, R.M., Horsrud, P., Raaen, A.M. and Risnes, R. 2008. *Petroleum Related Rock Mechanics*, 2nd edn. Elsevier.

Flechtner, F. and Aubele, K. 2019. A brief stock take of the deep geothermal projects in Bavaria, Germany (2018). Paper SGP-TR-214, presented at the PROCEEDINGS, 44th Workshop on Geothermal Reservoir Engineering, 11–13 February 2019, Stanford University, Stanford, California.

Gier, S., Ottner, F. and Johns, W.D. 1998. Layer-charge heterogeneity in smectites of I-S phases in pelitic sediments from the Molasse Basin, Austria. *Clays and Clay Minerals*, **46**, 670–678, https://doi.org/10.1346/CCMN.1998.0460607

IRENA 2017. *Geothermal Power - Technology Brief*. International Renewable Energy Agency (IRENA).

IRENA 2021. *World Energy Transitions Outlook*. International Renewable Energy Agency (IRENA).

Kuhlemann, J. and Kempf, O. 2002. Post-Eocene evolution of the North Alpine Foreland Basin and its response to Alpine tectonics. *Sedimentary Geology*, **152**, 45–78, https://doi.org/10.1016/S0037-0738(01)00285-8

Lackner, D., Lentsch, D. and Dorsch, K. 2018. Germany`s deepest hydro-geothermal doublet, drilling challenges and conclusions for the design of future wells. *Transactions - Geothermal Resources Council*, 349–359.

Lemcke, K. 1976. Übertiefe Grundwässer im süddeutschen Alpenvorland. *Bulletin der Vereinigung Schweiz. Petroleum-Geologen und -Ingenieure*, **42**, 9–18.

Lemcke, K. 1979. Dreissig Jahre Oel- und Gassuche im süddeutschen Alpenvorland. *Jahresberichte und Mitteilungen des Oberrheinischen Geologischen Vereins*, **61**, 305–317, https://doi.org/10.1127/jmogv/61/1979/305

Lüschen, E., Borrini, D., Gebrande, H., Lammerer, B., Millahn, K., Neubauer, F. and Nicolich, R. 2006. TRANSALP - deep crustal Vibroseis and explosive seismic profiling in the Eastern Alps. *Tectonophysics*, **414**, 9–38, https://doi.org/10.1016/j.tecto.2005.10.014

Mouchet, J.-P. and Mitchell, A. 1989. *Abnormal Pressures while Drilling: Origins, Predictions, Detection Evaluation*. Editions Technip, Paris, France.

Müller, M., Nieberding, F. and Wanninger, A. 1988. Tectonic style and pressure distribution at the northern margin of the Alps between Lake Constance and the River Inn. *Geologische Rundschau*, **77**, 787–796, https://doi.org/10.1007/BF01830185

NIBIS®Kartenserver 2019. *Geophysik und Tiefbohrungen*. Landesamt für Bergbau, Energie und Geologie (LBEG), Hannover.

Pasternak, M. 2011. Exploration and Production of Crude Oil and Natural Gas in Germany in 2010. *Erdöl Erdgas Kohle*, **127**, 272–286.

Pfiffner, O.A. 1986. Evolution of the north Alpine foreland basin in the Central Alps. *In*: Allen, P.A. and Homewood, P. *Foreland Basins*, Blackwell Scientific Publications, Oxford, UK, 219–228.

Pinkston, F.W.M. and Flemings, P.B. 2019. Overpressure at the Macondo Well and its impact on the Deepwater Horizon blowout. *Scientific Reports*, **9**, https://doi.org/10.1038/s41598-019-42496-0

Pletl, C., Angerer, J., Graf, R., Stoyke, R. and Toll, H. 2010. Bohrerfahrungen bei Deutschlands größtem Geothermieprojekt. *bbr - Leitungsbau, Brunnenbau, Geothermie*, **3**, 38–47.

Przybycin, A.M., Scheck-Wenderoth, M. and Schneider, M. 2017. The origin of deep geothermal anomalies in the German Molasse Basin: results from 3D numerical models of coupled fluid flow and heat transport. *Geothermal Energy*, **5**, https://doi.org/10.1186/s40517-016-0059-3

Reinecker, J., Tingay, M., Müller, B. and Heidbach, O. 2010. Present-day stress orientation in the Molasse Basin. *Tectonophysics*, **482**, 129–138, https://doi.org/10.1016/j.tecto.2009.07.021

Sachsenhofer, R.F., Leitner, B. *et al.* 2010. Deposition, erosion and hydrocarbon source potential of the Oligocene Eggerding Formation (Molasse Basin, Austria). *Austrian Journal of Earth Sciences*, **103**, 76–99.

Schmid, S.M., Fügenschuh, B., Kissling, E. and Schuster, R. 2004. Tectonic map and overall architecture of the Alpine orogen. *Eclogae Geologicae Helvetiae*, **97**, 93–117, https://doi.org/10.1007/s00015-004-1113-x

Schulz, I., Steiner, U. and Schubert, A. 2017. Factors for the success of deep geothermal projects – experience from the Bavarian Molasse Basin. *Erdöl Erdgas Kohle*, **133**, 73–79.

Sissingh, W. 1997. Tectonostratigraphy of the North Alpine Foreland Basin: correlation of Tertiary depositional cycles and orogenic phases. *Tectonophysics*, **282**, 223–256, https://doi.org/10.1016/S0040-1951(97)00221-7

Stefansson, V. 2002. Investment cost for geothermal power plants. *Geothermics*, **31**, 263–272, https://doi.org/10.1016/S0375-6505(01)00018-9

Stober, I. and Bucher, K. 2013. *Geothermal Energy: From Theoretical Models to Exploration and Development*. Springer-Verlag, Berlin, https://doi.org/10.1007/978-3-642-13352-7

Zweigel, J. 1998. Eustatic versus tectonic control on foreland basin fill: sequence stratigraphy, subsidence analysis, stratigraphic modelling, and reservoir modelling applied to the German Molasse basin. *Contributions to Sedimentary Geology*, **20**, X-140.